Changing resonator geometry to boost sound power decouples size and song frequency in a small insect

Natasha Mhatre[a,1], Fernando Montealegre-Z[a], Rohini Balakrishnan[b], and Daniel Robert[a]

[a]School of Biological Sciences, Woodland Road, University of Bristol, Bristol BS8 1UG, United Kingdom; and [b]Centre for Ecological Sciences, Indian Institute of Science, Bangalore 560012, India

Edited by A. J. Hudspeth, Howard Hughes Medical Institute, New York, NY, and approved March 28, 2012 (received for review January 6, 2012)

Despite their small size, some insects, such as crickets, can produce high amplitude mating songs by rubbing their wings together. By exploiting structural resonance for sound radiation, crickets broadcast species-specific songs at a sharply tuned frequency. Such songs enhance the range of signal transmission, contain information about the signaler's quality, and allow mate choice. The production of pure tones requires elaborate structural mechanisms that control and sustain resonance at the species-specific frequency. Tree crickets differ sharply from this scheme. Although they use a resonant system to produce sound, tree crickets can produce high amplitude songs at different frequencies, varying by as much as an octave. Based on an investigation of the driving mechanism and the resonant system, using laser Doppler vibrometry and finite element modeling, we show that it is the distinctive geometry of the crickets' forewings (the resonant system) that is responsible for their capacity to vary frequency. The long, enlarged wings enable the production of high amplitude songs; however, as a mechanical consequence of the high aspect ratio, the resonant structures have multiple resonant modes that are similar in frequency. The drive produced by the singing apparatus cannot, therefore, be locked to a single frequency, and different resonant modes can easily be engaged, allowing individual males to vary the carrier frequency of their songs. Such flexibility in sound production, decoupling body size and song frequency, has important implications for conventional views of mate choice, and offers inspiration for the design of miniature, multifrequency, resonant acoustic radiators.

bioacoustics | biological modelling | biomechanics | finite element analysis

Male crickets produce high amplitude calling songs to attract conspecific females (1, 2). The sounds are produced by stridulation, a rapid and controlled rubbing of forewings against each other. The plectrum, a sclerotized portion on the anal edge of one wing, is drawn across the file, a series of teeth on the underside of a vein, on the other wing (reviewed in ref. 3). The stridulatory apparatus acts as a mechanical frequency-multiplying system, converting the slow wing-stroke rate (*ca* 30 Hz) of the insect into a sound of much higher frequency (e.g., 4.5 kHz in the field cricket *Gryllus bimaculatus*) (3, 4). Stridulation sets the wing into vibration, and if the frequency produced by the plectrum-file interaction (the tooth strike rate) matches the resonance frequency of the wings a higher amplitude pure-tone sound can be produced (2). The exact biophysical mechanisms enabling such sound radiation using soft structures many times smaller than the sound wavelength remain elusive.

The mechanism that crickets use to match stridulatory frequency to resonant frequency is similar to a clockwork-like escapement system (5–7). In the field of horology, escapement mechanisms display different degrees of sophistication (8), one is even called the grasshopper escapement (9). The fundamental principle of an escapement can, however, be illustrated by the simple deadbeat escapement. In a deadbeat escapement, the resonant system is a pendulum that acts as a regulator and sets the speed at which the mechanism oscillates. The force comes from a rotating gear whose teeth engage and apply force to pallets attached to the pendulum. The sequential release of the gear teeth by the pallets allows the gear to move forward only once every oscillation by mechanically blocking its motion at other times. Hence, the frequency at which the gear tooth engages and imparts force back to the pendulum is set by the pendulum itself (8). Cricket wings play the same role as the pendulum by determining the dominant or carrier frequency (CF) of the cricket's song (5, 6), and the file and plectrum are the analogs of the gear and pallets parts of the escapement mechanism prompting the term "clockwork cricket" (5, 7). In the absence of such an escapement mechanism, the CF of a cricket song would be variable, and their wings would be much less efficient at producing high amplitude mate attraction signals (2).

Crickets are poikilothermic animals, and their physiology is greatly affected by changes in ambient temperature as is their song (10–13). In field crickets, where the escapement system is best studied, the song CF changes very little with temperature (6). As the resonant frequency of the wings does not change with temperature, it was proposed that the plectrum cannot proceed along the file any faster despite the overall change in the speed of the wing-stroke (5, 6). As a result, the song CF does not change, and crickets can produce high amplitude, pure-tone signals regardless of ambient temperature (6).

Another implication of this deterministic mechanical model of sound production is that there is an inflexible relationship between body size and song CF within a species of cricket (4, 14, 15); hence, CF is an obligatorily honest signal of an individual's size. Moreover, all insects that use similar sound production mechanisms such as katydids (tettigoniids) and field crickets (gryllids), were expected to follow this pattern (4). Earlier research showed that females prefer males broadcasting lower CF songs; hence, females choose larger and potentially fitter males (16–18). The generality of this mechanism for female choice has been challenged in birds and mammals (19, 20) but not in insects. Examples of uncoupling CF from size is rare in insects; yet, a notable exception are the Oecanthines, or tree-crickets, whose calling song CF varies greatly with temperature (10, 21, 22).

Tree crickets (Oecanthinae, Gryllinae, Orthoptera) are distinguished by beautiful, transparent wings that are conspicuously enlarged with respect to their body size (22–25). Little is known, however, about the relationship between temperature, the stridulatory mechanism, and wing resonances in Oecathines (23, 26). Even less is known about the evolutionary reasons for their remarkable wings and the consequences of having sound radiators that are so different from those of the previously studied field crickets (27, 28) and katydids (29, 30).

The key outstanding question pertains to the mechanism that enables the production of variable frequency songs that are high amplitude and tonal. We dissect the relationship between the

Author contributions: N.M., F.M.-Z., R.B., and D.R. designed research; N.M. and F.M.-Z. performed research; N.M. and F.M.-Z. analyzed data; and N.M. wrote the paper.

The authors declare no conflict of interest.

This article is a PNAS Direct Submission.

[1]To whom correspondence should be addressed. E-mail: natasha.mhatre@bris.ac.uk.

This article contains supporting information online at www.pnas.org/lookup/suppl/doi:10.1073/pnas.1200192109/-/DCSupplemental.

forces generated by the stridulatory mechanism, and the resonant behavior, size and shape of the acoustic radiators. The results reveal that the ability to produce variable frequencies is determined by morphological geometry; i.e., the high aspect ratio of the resonator. The results also suggest that the evolution of this wing morphology is driven by the need to produce higher amplitude mate attraction songs, and the variable frequency is an inevitable outcome. In biophysical terms, the results uncover a remarkably simple method to design efficient resonators with variable frequency output. The other interesting outcome *vis a vis* sexual selection is that it negates the idea that insects are obliged to signal their body size honestly as a result of their inflexible sound production mechanism.

Results

The "Ticking" in Tree-Cricket Song. It has been suggested that if stridulation relies on an escapement mechanism, the plectrum will make a high frequency 'ticking' sound as it engages each tooth of the file (7). The ticking that is produced is soft; yet, it is expected to produce small irregularities in the acoustic waveform. Close examination of song recordings made in the field from the South Indian tree cricket *Oecanthus henryi* (22) reveals the presence of small and regular variations in the instantaneous frequency (7). These can be observed in *O. henryi* songs recorded at different temperatures (Fig. 1).

The ticking signature of the escapement mechanism can also be recorded and examined over the longer time course of a complete syllable made during a single closing stroke. It is expected that the amplitude envelope of the higher frequency (HF) ticking component of the syllable will be different from that of the lower frequency CF component because the amplitude of the drive changes over time (7). Alternatively, if the two envelopes correspond exactly, it is expected that the HF elements are a product of harmonic distortion and not produced by the stridulatory apparatus. We found that the envelope of the HF ticking sound was different from that of the CF sound as can be observed in the time resolved gain between the unfiltered and filtered syllables over a range of temperatures (Fig. 1). Remarkably, the temporal dynamics of instantaneous frequency and HF components change with temperature (Fig. 1).

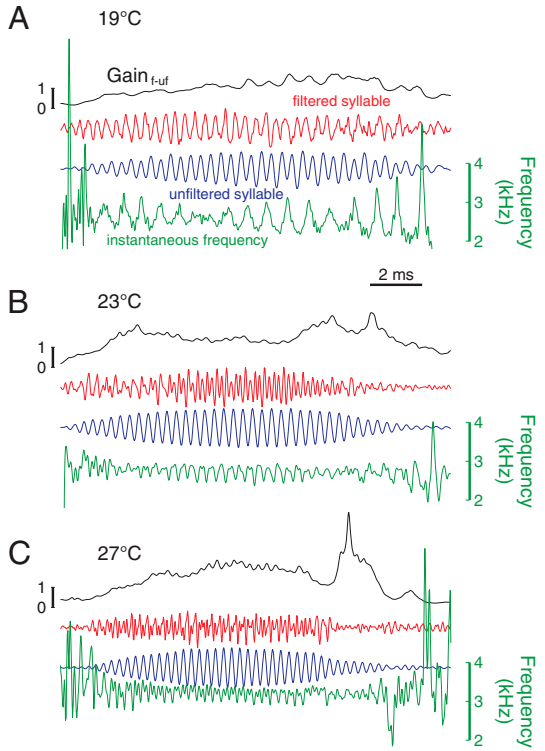

Fig. 1. Time-resolved frequency analysis of *O. henryi* song and the ticking of stridulation. A syllable of song produced by an *O. henryi* male singing (blue trace) at (*A*) 19 °C, (*B*) 23 °C, and (*C*) 27 °C. All songs show a Hilbert instantaneous frequency (green trace) that varies regularly on a cycle-by-cycle basis. Removing the low frequency components of the song reveals the envelope of the high frequency components (red trace). This component shows an amplitude envelope that is distinct from the main sound pulse as shown by the gain calculated between them (black trace).

Modeling the Stridulatory Apparatus. Having found evidence for an escapement mechanism in *O. henryi* songs, the next step was to probe the nature of the mechanical drive imparted to the wings. Three models of the forces that developed during the closing stroke of stridulation were generated. Each model had a different force regime: a sinusoidal drive, an impulsive drive, and a "catch and release "drive (Fig. 2*A*). The latter two have been the dominant models in describing an escapement system in field cricket stridulatory behavior (6, 31).

With all three models, because there is a net positive force on each wing through time, a net forward movement of the plectrum along the file will be produced (Fig. 2*B*). When the displacement of the wing is high-pass filtered to remove the low frequency component, the cyclic regular displacement caused by each tooth strike can be observed more clearly (Fig. 2*C*). When this filtered signal is plotted against the sound that is produced by the system,

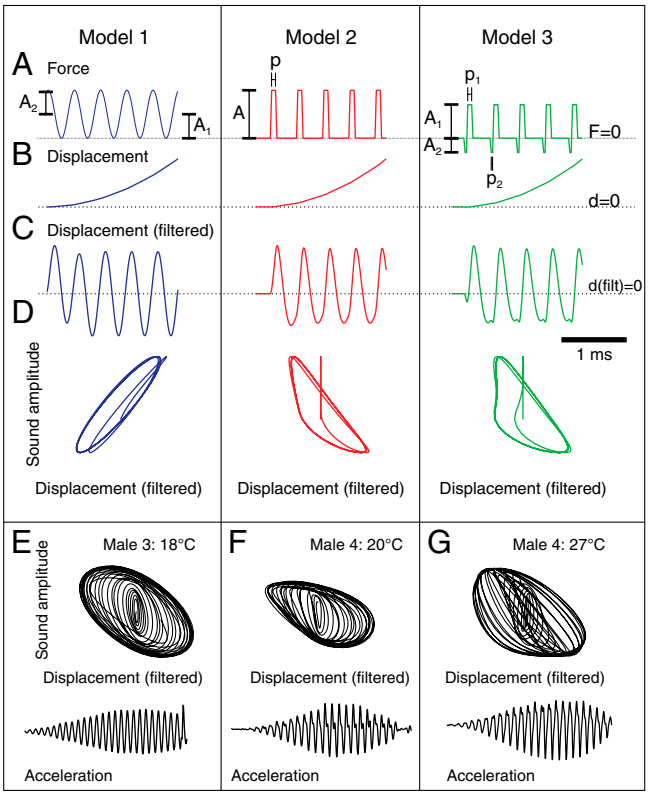

Fig. 2. Three escapement models for stridulation and comparison with experimental data. The three models are described in terms of oscillograms of (*A*) the forces applied by the stridulatory apparatus, (*B*) displacement of the wing along the file because of these forces, (*C*) the displacement time series when filtered for the steady forward movement, and (*D*) Lissajous plots of the filtered displacement vs. the sound amplitude produced. Lissajous plots of the filtered displacement of the wings during a single closing stroke against the sound produced show the presence of all three drive models, model 1 (*E*), and model 2 and 3 (*F* and *G*) occurring in a single pulse at different amplitudes and times within the pulse. The compression produced in model 3 was observed only for two cycles at the beginning of the pulse shown in (*G*).

with an arbitrary and constant phase delay, the three force regimes yield clearly different signatures (Fig. 2*D*). The sinusoidal drive produces a simple elliptical shape such as would be expected from a single frequency input and output system (Fig. 2*D*). The impulsive force and the catch and release models produce distinct characteristic triangular-shaped Lissajous plots (Fig. 2*D*). The catch and release model reveals an additional compression due to the effect of the periodic negative force (Fig. 2*D*).

When equivalent Lissajous plots were constructed using data from *O. henryi* males singing at different temperatures, all three patterns were observed (Fig. 2 *E*, *F*, *and G*). A simple elliptical shape such as that produced by the sinusoidal drive model is seen in a low temperature recording (Fig. 2*E*). The changing axis of the ellipse in this figure indicates that the relative phase between sound and drive changes during the course of the pulse (Fig. 2*E*). At higher temperatures, occasionally triangular Lissajous plots were produced, and they show the presence of higher harmonics introduced by the impulsive nature of the drive (Fig. 2 *F* and *G*), as noted in a similar analysis before (6). These higher harmonics can be observed to increase in relative amplitude at the higher temperatures (see Fig. S1).

During a closing stroke, the net force between the two wings never falls to and remains at zero (Fig. 2 *E*, *F*, *and G*). In a true escapement, if the drive attempted to move faster than the speed set by the resonance frequency, it would periodically be brought to a complete halt and allowed to proceed only at a rate that produced the appropriate frequency. Although higher harmonics are present in the net force between the wings, the wings are never brought to a complete halt. These data lead us to conclude that the wings are moving at speeds below that set by the resonance, or *O. henryi* does not have a true clockwork-like escapement system.

Because the *O. henryi* system behaves differently, we decided to investigate the effect of temperature on the tooth strike rate. We found that when ambient temperature increases, individual tree crickets increase the speed of their wing stroke cycle including the closing stroke (Fig. 3*C*). This increase in wing speed leads to an increased tooth strike rate with increasing temperature that, in turn, leads to a higher song CF (Fig. 3*D*). This increase in the speed of the closing stroke (1.9 times per °C) appears to be lower than the increase seen in the syllable repetition rate [2.27 times per °C, computed from data in (22)] suggesting that the speed of the closing stroke is impeded by engagement with the stridulatory apparatus, though it is not kept at a temperature independent constant velocity as would be predicted by a pure escapement model.

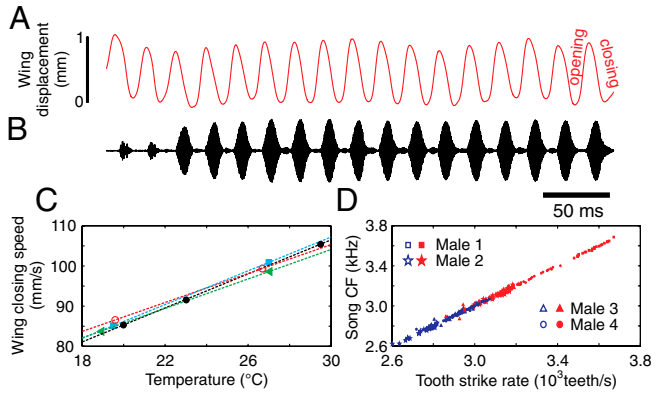

Fig. 3. Wing movements during stridulation and temperature dependence. (*A*) Wing movements recorded during singing show that the associated sound pulses (*B*) in a chirp are produced mainly during the closing stroke while the opening stroke is silent. (*C*) The average speed of the closing stroke increases linearly with temperature (each symbol represents an individual). (*D*) Song CF also increases linearly with tooth strike rate resulting in higher CF at higher temperature. Each symbol represents an individual, and the different data points for each individual were for multiple syllables from each individual. Low temperature recordings are represented by blue symbols (Males 1–4: 22.1 °C, 18.5 °C, 22.9 °C, and 21.1 °C) and high temperature by red symbols (Males 1–4: 28.0 °C, 25.4 °C, 25.3 °C, and 26.6 °C).

Resonance in *Oecanthus henryi* Wings. In tree crickets, CF and stridulatory drive changes with temperature raising the question of whether wing resonances are temperature dependent. To characterize the resonances in *Oecanthus* wings, the wings of eight males were scanned with a laser Doppler vibrometer while being immobilized in the singing position (see Fig. S2). The wings of *O. henryi* vibrated maximally and most coherently in response to sound between 2.5 and 4.5 kHz at all temperatures (Fig. 4). This broad frequency response covers the natural range of carrier frequencies produced by singing males (2.3 to 3.7 kHz, Fig. 2) (22). The main peak within the broad vibratory response shifts slightly with increasing temperature, and higher frequencies produce greater displacements at higher temperatures; however, the broad response pattern is not altered (Fig. 4*A*). Such a low Q resonator with a broad frequency response makes for a poor radiator of sound in addition to producing variable song CFs.

In order to understand the reasons for this frequency response, different parts of the wings were assessed for their relative contributions to the overall frequency response. The phase and amplitude of the displacement of different parts of the wing were plotted for different temperatures. Central scan points were selected from the following wing areas: the anal field (*A*), the harp (*H*), the first, second, and third mirror cells (*M1*, *M2* and *M3*, respectively) (Fig. 5; Fig. S3). Except for the anal field (*A*), all areas of the wing respond with nearly equal displacement amplitudes between 2.5 and 4.5 kHz (Fig. 5) unlike in field crickets wings in which the harps contribute the most to the frequency response (28, 32). The phase response of the transfer function begins near 90° at about 2.5 kHz and falls to near −90° at about 5 kHz (Fig. 5). The decrease from 90° to −90°, however, is not monotonic and, interestingly, shows a step-like shape that is most prominent in the harp and M1 response. The first part of the phase transition corresponds to the first peak within the broad frequency response, observed most clearly in the lowest temperature measurements (Fig. 4). The second part of the transition betrays the second peak in the frequency response (Fig. 4). The fine structure of the phase transition thus reveals the presence of two deflection modes in *O. henryi* wings that are set at very similar frequencies.

The deflection shapes of the wings show the two modes that occur at the two peaks in the frequency response. In the first mode (1, 1), set at the lower frequency, the harp and mirrors

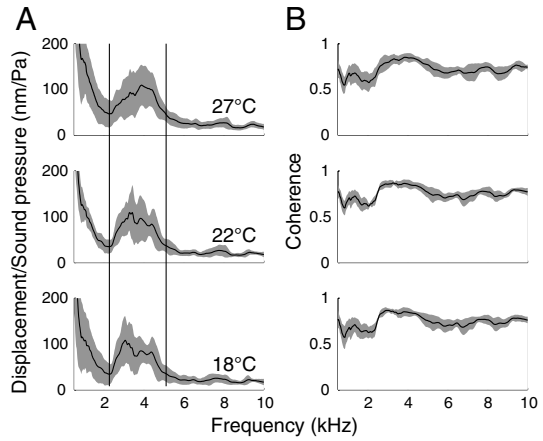

Fig. 4. Frequency spectra of (*A*) the displacement amplitude and (*B*) coherence averaged across both wings measured at three different temperatures. The bold lines depict the mean, and the shaded area depicts the standard deviation, $N = 8$ males.

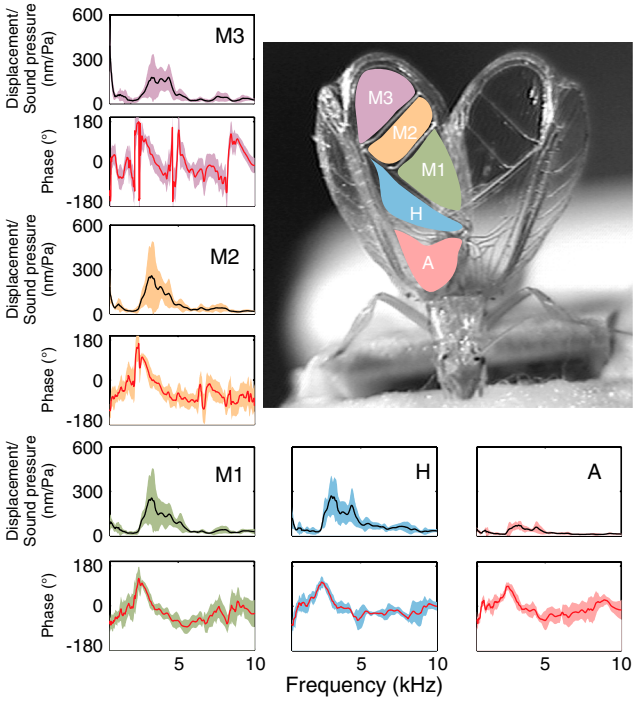

Fig. 5. The amplitude and phase of the displacement transfer function of different wing areas (color coded) at 18 °C. The anal field (*A*) moves the least as expected because it is closest to the wing hinge. At the central points, all other areas of the wing, the harp (*H*), and mirrors 1, 2 and 3 (*M1, M2, M3*) respond with nearly equal amplitudes. Data from both wings at all temperatures are presented in Fig. S3.

vibrate in phase with each other (from left wing harps: $f_{(1,1)} = 3.04 \pm 0.355$ kHz, $Q = 12.31 \pm 6.33$) (Fig. 6*A*, *B*, *E*, and *F*). In the second mode (1, 2), the harp and M1 vibrate out of phase with M3 with clear bending occurring within M2 (from left wing harps: $f_{(1,2)} = 4.315 \pm 0.454$ kHz, $Q = 11.03 \pm 7.36$) (Fig. 6 *C*, *D*, *G*, and *H*). Although the relative displacement amplitude of the two wings varies between individuals, on average, across the sample no systematic asymmetry exists in either mode (Fig. 6 *E*, *I* and *G*, *K*).

Both modes are similar to each other, displaying similar deflection magnitudes and phases across the wing (Fig. 6 *I*, *J*, *K*, and *L*). In particular, the phase remains close to 0° (Fig. 6 *J*, and *L*) between the two peaks in displacement response (Fig. 5). The phase difference reveals that the time delay between input and output (i.e., the tooth strike and the wing deflection) is small and does not differ greatly between the two modes. Because the input and output occur with nearly 0° phase difference, the energy imparted by the strike to the wing will be synchronous with the upward wing deflection. This synchrony allows the plectrum to impart energy to the wing in a direct and efficient manner, more so than at any other phase of its cyclical motion. An analogy often made to describe such an oscillatory situation is pushing a child on a swing: the best time to push, in order to impart energy efficiently, is when the swing is at the end of its motion towards the pusher in a brief stationary state. Thus, by keeping the phase near 0°, the two modes allow efficient and rhythmic capture and release of the teeth at a wider frequency range than would be possible with a single broadband resonator.

The Importance of Wing Geometry and Aspect Ratio. The entire wing shows a clear vibratory response near song CF when stimulated by sound (Fig. 5), and it is the long, nearly elliptical shape of the wing that turns out to be key to its frequency response. We used a finite element (FE) model to investigate the effect of shape on the resonant behavior of plates designed to have the same geometry and structure as the wings. The geometry of these plates was then varied by changing their aspect ratio *Ro* (or length to width ratio). Three cases were considered for analysis: (*i*) the natural geometry (Fig. 7*A*), (*ii*) $0.5^{*}R_o$ (Fig. 7*B*), and (*iii*) $1.5^{*}R_o$ (Fig. 7*C*). The first two vibratory modes for all three wing models

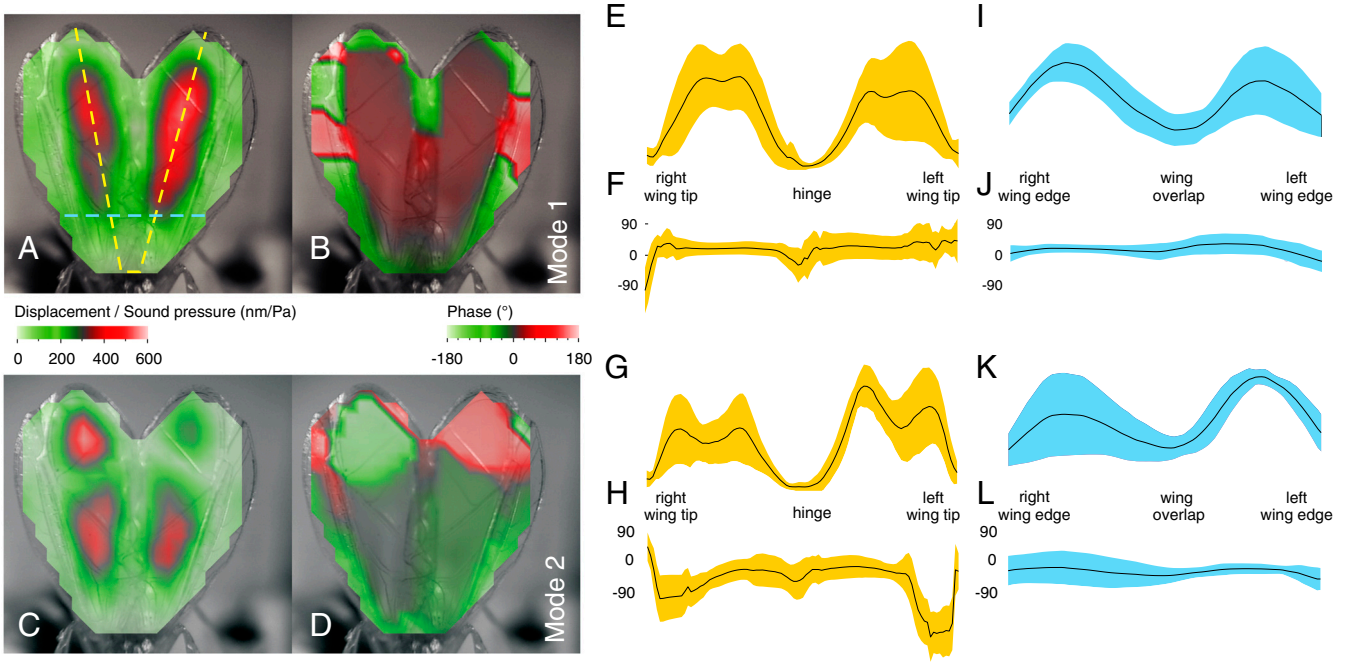

Fig. 6. Deflection modes in wing resonators. Example of a male whose wings had the first mode (1, 1) at a frequency of 3.4 kHz (*A*) where the entire wing vibrated in phase (*B*). The second mode occurred at 4.2 kHz (*C*, *D*) where the harp and M1, vibrated out of phase with M3, and an antinode was formed in M2. Measurement taken at 27 °C. To describe these modes across all males, two transects were defined (as shown in *A*), and the normalized deflection amplitude (*E* and *I*: mode 1; and *G* and *K*: mode 2), and phase (*F* and *J*: mode 1, and *H* and *L*: mode 2) were measured along these transects (18 °C). The mean value is shown by the dark line, and the shaded areas describe the standard deviation. Colors of shaded areas (*E*–*L*) match that of the transect (*A*).

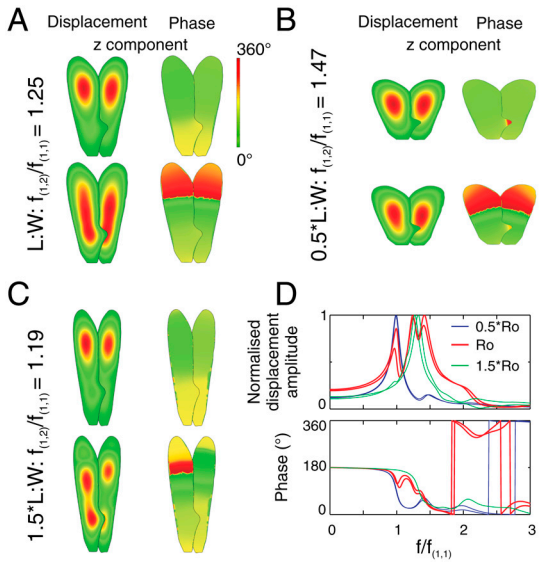

Fig. 7. Deflection modes in comparative FEM models. Models of *O. henryi* wings with a natural aspect ratio (Ro) (*A*) have their first two modes at a ratio of 1:1.25 that corresponds closely to the real wing resonance (1:1.37), whereas wings with a lower aspect ratio ($0.5^{*}R_o$) (*B*) have them at a ratio of 1:1.47. (*C*) Further elongating the wings, ($1.5^{*}R_0$) causes the two modes to move closer together (ratio: 1:1.19). (*D*) The amplitude and phase of the normalized frequency response of the wings reflect this mixing of the modes. The frequency response of the modeled wings were measured at the harps, and the two traces represent each wing separately.

were quite similar to the (1,1) and (1,2) modal displacement shapes and phases seen in the real wings (Fig. 6, 7).

In terms of frequency ratio of the first two modes, however, the highest ratio was achieved by the shortest wings, and the lowest ratio was achieved by the longest wings (Fig. 7 *A*, *B*, and *C*). The average ratio of the two modes in the real wings is $1:1.37 \pm 0.06$ (mean $\pm$ SD, range = 1:1.28 to 1:1.44). The combination of the $f(1,2):f(1,1)$ ratio and relative amplitudes of the two modes closest to that of the real wings was achieved by the natural aspect ratio plate model (Fig. 7 *A*, *B*, and *C*). For wings with a natural aspect ratio, the first two modes measured at the harp are similar in frequency and amplitude responses (Fig. 7*D*). In shorter wings ($R_o < 1$) resembling the resonant structures of field cricket wings, the first and second modes differ greatly in frequency and in displacement amplitude (Fig. 7*D*). In longer wings, the first three modes merge together entirely, and their amplitudes cannot be considered separately (Fig. 7*D*). This analysis reveals that, *ceteris paribus*, it is the geometrical aspect ratio of the wings that strongly influences their frequency response by causing modes to merge in the frequency domain thus enabling the broad frequency response observed in the wings of *O. henryi*.

Discussion

Resonances and the Consequences of Wing Aspect Ratio. During stridulation, the wings of crickets, when set in motion by the action of the stridulatory apparatus, vibrate and produce pressure variations in the surrounding medium effectively producing sound (3). Sound radiation using wings has been studied in many groups in the singing Orthopteran insects: bush crickets (30), crickets (27, 28, 32) and tree crickets (23). In most crickets, only part of the wing (the harp or the mirrors) moves significantly and radiates sound at the song CF (27, 30, 32). Unusually, in *O. henryi* the entire wing (the harp, and the three distal wing mirrors) shows significant vibrational behavior (Fig. 6 *A* and *C*), which produces a very low frequency song varying between 2.3 and 3.7 kHz (Fig. 3) (22). This conversion of the entire wing into a resonator for acoustic radiation has important consequences for its frequency response.

When the entire wing is used for sound radiation, the shape of the effective resonant plate is significantly elongated along the length of the wing in comparison with the triangular harp, which has a smaller aspect ratio. Given that the elongated resonator shape is peculiar to Oecanthines that produce calls with variable CF, we used an FE modeling approach to investigate the effect of wing geometry on the relative frequency of the resonant modes. A simple feature of wing geometry, the aspect ratio was found to influence two important aspects of the wing vibration: the frequencies of resonant modes and their relative amplitude. A low aspect ratio increased the distance in frequency between the first and the second modes, and it decreased the relative amplitude of the second mode (Fig. 7*D*). A high aspect ratio resonator, such as that seen in real wings, brings the first two modes closer together in frequency and it equalizes their amplitudes (Fig. 7*D*). Following the inclusion of damping, as measured by our vibrometry experiments, we found that the modes merged into each other in the frequency domain. It is this broad frequency response that allows the stridulatory apparatus to move seamlessly from one mode to the other during song production. The wing speed determines the mode that is engaged, and this causes a change in CF at different temperatures. The proximity of the modes is also important in allowing the drive to be input in a phase-coherent manner over a broad range of frequencies (Fig. 6 *J* and *L*).

Other Oecanthine species share the peculiar high aspect ratio wing morphology of *O. henryi* (22–25); hence, we would expect similar mechanical behavior in other tree crickets. Based on our FE models, we proposed that it is the high aspect ratio of the resonant structure in the Oecanthine wing that causes the temperature dependent CF change seen in songs across the genus. Crickets with lower aspect ratio resonators are expected to produce sound at only the first mode and be more sharply tuned; hence, they would have a frequency invariant song as exemplified by field crickets.

In our FE model, an important simplifying assumption is made. The model ignores the contribution of the veins that lie within the resonating structure of the wing, and it ignores the effects of subtle fluting observed within the wing cuticle. Both these features of the wing's structure are expected to increase its stiffness in an anisotropic manner; i.e., the stiffness would increase only in the direction of the vein or fluting axis (33). The contribution of these features to wing vibration will be the subject of future investigation. Despite ignoring the influence of these features, a simplified model is able to reproduce the modal shapes closely and the relative frequency response of the wing. In effect, the subtle fluting features of the plate are not expected to alter the primary modes completely. Lower modes arise due to longer flexural waves that travel unimpaired through smaller structures and were immune to local effects (33, 34). This resilience is corroborated by the observation that damaged wings show primary modes similar to those of undamaged wings (see Fig. S7).

Stridulatory Models and Temperature-Dependent Carrier Frequency. The broad frequency response of the wings is germane to the driving force produced by the stridulatory apparatus. Based on the escapement model, it was suggested that from very low temperatures to mid range temperatures, the CF of song increases in field crickets; however, at a certain point when the CF reaches the wing resonance frequency the wing resonance steps in and, using a clockwork-like escapement mechanism, prevents the plectrum wing from going any faster, thus effectively preventing an increase in song CF (6). To investigate the relevance of this model in *O. henryi* song production, we investigated field recordings of *O. henryi* song using the sensitive Hilbert transform to look for evidence of an escapement system. We found cycle-by-cycle variations in the instantaneous frequency of song (Fig. 1) as would be produced by the impulsive engagement and release of file teeth (7). We also found that the softer, higher harmonics in the songs

did not have the same amplitude profile as the sound pulse, i.e., the gain between the high frequency and low frequency components of the sound pulse builds up over time as expected for a driven resonant system (Fig. 1).

The higher harmonics observed here in *O. henryi* song are not similar to the ultra subharmonics observed in the *O. nigricornis song* that are only present transiently (26) and that can be explained by sound radiation by the higher modes that are not harmonically related. Regular increases in instantaneous frequency observed here (once each CF cycle) are consequences of the file teeth being engaged by the plectrum. This change in frequency is a reasonable expectation as each CF cycle in a syllable is known to correspond to a tooth in the file (23, 26).

Direct measurements of the wing positions (Fig. 3*A*) allowed us to calculate the time course of the effective force applied to the wing during a closing wing stroke. We developed three models of the force regimes applied to the plectrum wing moving over the file of the opposite wing: (*i*) a null model of a sinusoidal force, (*ii*) an impulsive force, and (*iii*) a catch and release model (Fig. 3). These models allow comparison of data in the time (Lissajous plots) and frequency domain (higher harmonics in the spectrum) (see Fig. S1). The catch-and-release model, and the impulsive force models for stridulation described here, are possible only in a situation where some external input first prevents the plectrum from moving continuously over the file, and then it allows it to release the file teeth in a regulated manner. Such impulsive force models are believed to be clearly indicative of a clockwork mechanism where the external input is deemed to be the wing resonance (5, 6). The sinusoidal model presents the case where the plectrum moves over the file, and it is only partially impeded through frictional forces as opposed to being brought to a complete halt as in the other two models (Fig. 3).

Surprisingly, we found that the wings of singing *Oecanthus henryi* males did not conform to a single model. Instead, many measurements fit the sinusoidal force model (Fig. 3*E*) and other measurements fit both escapement models (Fig. 3 *F* and *G*). We found evidence for the catch and release and the impulsive force model in a single sound pulse (Fig. 3 *F* and *G*). This evidence demonstrates that different modes of escapement are possible within a single system and, the singing of a tree cricket is truly anything but "clockwork."

The presented data on the stridulatory mechanics in *O. henryi* show that the wings are never brought to a complete halt by the wing resonance. The speed of the plectrum across the file is influenced, though not entirely determined by, the wing resonance as would be suggested by the clockwork model (5, 6). As a result, the speed can be influenced to a greater degree by other factors. Ambient temperature increases the activity of muscles and the motor neurons innervating them in poikilotherms, and is expected to cause an increase in the wing speed (10, 12, 35–38). In *O. henryi*, we found that the wing speed and, hence, the rate at which teeth within the file are struck, increases linearly with ambient temperature above the center frequency of the first resonant mode (Fig. 3 *C* and *D*). These observations clearly demonstrate that the drive frequency is not specified by the first resonant mode of the wings. Because the driving force can be delivered at a higher frequency, it can begin to engage the second resonant mode of the wing. Because the first and second modes are quite similar in frequency, the CF of the *O. henryi* song can and does increase with increasing temperature (Fig. 3 *C* and *D*).

The Reasons for Increasing Sound Radiator Size. The wings of a cricket are not just the pendulum in the clockwork cricket, they are also the primary radiators of sound (2, 3). So, why is the entire wing converted into the resonant structure in Oecanthines as opposed to just the harp or the mirrors? We argue that this is a consequence of the phylogenetically constrained size of tree crickets. Tree crickets are small especially in comparison with other crickets and katydids (22). The area of the harp in *O. henryi* is only 2.61 ± 0.26 mm^2 (mean $\pm$ SD, $N = 6$), and the entire resonating structure in each wing is 17.07 ± 0.73 mm^2 (mean $\pm$ SD, $N = 6$). The entire wing of *O. henryi* is comparable in area to the harp of the *Gryllus bimaculatus* wing (16). If *O. henryi* used only the harp for sound radiation as opposed to the entire wing, then the area available for sound radiation would be smaller by more than a sixth.

The consequences of having a smaller or larger sound radiator are complex. The acoustic power radiated by the entire wing or harp is a function of the velocity of the wing resonance during singing and the radiation resistance it experiences (39). Based on our measurements and models, we estimated that the power radiated by entire wings is greater by a factor of 2.4 than the power produced by harps alone (see *Materials and Methods*). Hence, we can conclude that the change in shape is at least partially driven by a need to produce greater sound power, increase the range of acoustic communication, and enhance mate attraction (40, 41).

In addition to radiated sound power, there are other factors that can influence the CF at which crickets call (4). A powerful influence on song characters is the natural environment (42). Sounds of lower frequency travel further in cluttered environments and are less directional (42). *O. henryi* and other tree crickets are found mostly on bushes and, sometimes, in tall grasslands; hence, they are found in cluttered environments where a low frequency song is advantageous. This environmental constraint clearly favors the evolution of larger rather than smaller resonators.

Because the enlarged wing morphology is common to all Oecanthines, we speculate that not only *O. henryi*; but, all Oecanthines have been evolutionarily driven to use the entire wing as a sound resonator in order to produce a sufficiently high power and low frequency sound call suited to their environment. The use of the entire wing, however, has consequences for the resonant capabilities of the wings, and the result of this complex interplay of phylogenetic limitations to body size, physiology, and environmental acoustics is that male Oecanthines change the CF of their song with temperature.

The Consequences of Increasing Sound Radiator Size. The variation in song CF in tree crickets is a consequence of using the entire wing with its distinctive shape and size as a sound radiator. As a consequence of this song production mechanism, an increase in closing stroke wing velocity is possible, and individual tree crickets can vary their CF when ambient temperature changes. This mechanism opens the enticing, but unstudied possibility, that males can deliberately vary the CF of their calls independent of temperature by calling with greater wing velocity.

This behavior would have two consequences *vis a vis* sexual selection theory: first, it would break the direct link between body size and song CF. For instance, under natural conditions temperature gradients between different singing males would make it impossible for females to reliably identify the size of the males from their CF alone. Because an individual can simply call from a region of lower temperature in order to exaggerate its apparent size, song CF is no longer an obligatorily honest signal. In exactly the same vein, an individual could also produce lower wing velocities and hence, CFs in order to sound larger.

The second consequence of the ability to break the link between song CF and body size is that it may allow the CF to be used as a reliable cue for immediate physiological condition. Males may actually be advertising their ability to produce a high wing velocity through a high CF. This speculation is in agreement with recent experiments that suggest that male size does not influence female mate choice in tree crickets (43), and other considerations such as recent diet and ability to provide a large nuptial gift might play a greater role (43, 44). Another alternative is that males may be advertising the temperature of their calling sites (45) which may in itself be a resource on which to raise a poikilothermic brood (46).

We conclude that it is only by considering the mechanistic basis of the sound production in tree crickets that we can understand how variable CF song is produced and begin to elucidate the evolutionary reasons that underpin it. Knowledge of the mechanism opens up the possibility that an insect can be flexible in its acoustic signaling behavior, opening up exciting questions in the area of sexual selection.

Materials and Methods

Analysis of Song Data. Song data collected from wild singing males reported previously (22) were analyzed to reveal the details of their spectral and magnitude composition. We examined the songs of *O. henryi* males for instantaneous frequency variations during the course of a single syllable using the Hilbert transform (47), which allows the sensitive computation of instantaneous frequency at the sampling rate. It is also conjectured that the magnitude envelope of the "ticking" would be different from that of the song itself (7) Each of the songs were high-pass filtered from 1.5 X CF using an elliptical filter (Rp: peak to peak ripple: 0.5 dB, Rs: stop-band attenuation: 20 dB) implemented in Matlab v7.10. The envelope of the normalized filtered song or putative drive (ε_f) was compared to the normalized unfiltered song (ε_{uf}) by computing an instantaneous gain ($G_{f\text{-}uf}$) that was then smoothed for presentation.

$$G_{f\text{-}uf} = \varepsilon_{uf}/\varepsilon_f. \quad [1]$$

Animals. *O. henryi* males were maintained singly at 26 °C with ad lib access to food and water under a 12 h:12 h day: night cycle. For the laser vibrometry experiments, males were mounted ventral side down and ventrally glued to a rectangular brass bar (5 × 1 × 60 mm), using liquid latex (Magnacraft) (see Fig. S2). The brass bar was connected to a metal rod (150 mm long, 8 mm diameter) by a thumbscrew that allowed the animal to be oriented into the required position. The animal could drink from cotton wool soaked with sugar water during the experimental procedure. The tegmina of the animal were raised as in the singing posture and glued in place with two small drops of nail polish applied to the wing base and metathorax. The anal area of the wing, where the drop was applied, is highly veined and does not vibrate significantly; hence, it is not believed to be involved in song production (26). For measurements of the stridulatory wing movements, animals were released and allowed to move freely on *Lantana camara*, a host plant in their natural habitat. Measurements were taken from the anterior view.

Stridulatory Wing Movement Recordings. Stridulatory wing movements and associated sound production were simultaneously recorded from four males at low and high temperatures. Sound production was monitored with a 1/4-inch (6.4 mm) precision pressure microphone (Brüel and Kjær, 4138). Wing movements were recorded using an optoelectronic device (30). A small piece (<0.25 mm^2) of reflective tape (Scotchlite 7610 and 8850 retro-reflective tape; Motion Lab Systems Inc.) was placed on the forewing, and its position was monitored with a photodiode. The reflective tape (0.5 × 0.5 mm) was attached to the left wing in a manner that allowed movements to be recorded in the anterior view perpendicular to the plane made by the wings of the singing cricket. Sound and wing-movement signals were recorded on separate channels of a computer data acquisition board at a sampling rate of 100 kHz (NI 9215, National Instruments UK Ltd). Tooth strikes were then isolated from the wing motion by band-pass filtering (1–7 kHz) the wing movement trace. Isolated tooth strikes were used to study the phase relationship between tooth impacts and sound vibration using Lissajous diagrams. The temperature was measured using a Testo 110 thermocouple digital output precision thermometer accurate to 0.2°C) (Testo Ltd).

Modeling the Stridulatory Mechanism. Time series of the wing positions were used to investigate three models of the forces acting during stridulation. The first null model is a sinusoidal force model where the plectrum moves along the file driven by a combination of a steady positive force and a sinusoidal force that occurs as it engages the file at regular intervals ($T = 1/f$) with positive indicating direction along the file, and negative indicating a backward movement. The frequency of the sinusoidal drive ($f = \omega/2\pi$) was determined by the tooth strike rate. The forces acting on the wing during the closing stroke are given by:

$$F(t) = mA_1 + mA_2 \sin(\omega t). \quad [2]$$

Where A_1 is the acceleration caused by the steady force, and A_2 is the amplitude acceleration caused by the sinusoidal force and the effective mass (m).

The second and third are escapement models extended from the equations described by Koch, et al., (6). In the second model, the file and the plectrum apply equal force causing net force and displacement to be zero. Periodically, due to escapement allowed by the wing resonance, the plectrum exerts an impulsive force F for a time $2\Delta t$ on the file at regular intervals whose period is ($T = 1/f$), and it is determined by the tooth strike rate. This periodic impulsive force can be modeled using a Fourier series for a rectangular pulse (47).

$$F(t) = mA_1\left(p + \frac{2}{\pi}\Sigma_{n=1}^{\infty}\frac{1}{n}\sin(n\pi p)\cos(n\omega(t+\phi))\right). \quad [3]$$

The parameters for this function are the amplitude of the positive force (A), the duty cycle of the positive force with respect to the zero force state of the function (p, where $p = 2\Delta t/T$), and frequency (f) as determined by the wing resonances. From this equation, we also know the expected ratios of the harmonics in the Fourier series.

In the third model, the impulsive force is first in the negative direction and then switches to the opposite positive direction. It has been suggested that the capture of the plectrum by the angled file requires "unhooking" before forward motion is possible. This unhooking is said to be achieved by the buckling of the plectrum (48). The negative force models the force produced by the unhooking or buckling motion and the usual forward force. These forces can be modeled using two rectangular pulses in opposite directions.

$$F(t) = mA_1\left(p_1 + \frac{2}{\pi}\Sigma_{n=1}^{\infty}\frac{1}{n}\sin(n\pi p_1)\cos(n\omega(t+\phi_1))\right) - mA_2\left(p_2 + \frac{2}{\pi}\Sigma_{n=1}^{\infty}\frac{1}{n}\sin(n\pi p_2)(\cos n\omega(t+\phi_2))\right). \quad [4]$$

The parameters to be estimated were the duty cycle of the positive force (p_1), the duty cycle of the negative force (p_2), and the amplitudes of the positive and negative impulses (A_1 and A_2). The frequency of these impulsive forces is determined as before.

In order to examine the real stridulatory behavior with respect to this model, we numerically double differentiate the forward displacement of the wing measured by the position detection system to acquire the wing acceleration. Assuming the effective mass of the system remains constant, we compared the acceleration data to the three models.

Laser Vibrometry. ***Experimental setup.*** Vibrometry experiments were carried out on a vibration isolation table (TMC 784-443-12R; Technical Manufacturing Corp.). The vibration isolation table and the experimental setup on it were placed in an acoustic isolation booth (IAC series 1204A; 4.50 × 2.25 × 1.98 m; Industrial Acoustics). Vibration velocities were measured using a microscanning laser Doppler vibrometer (Polytec PSV- 300-F) with an OFV-056 scanning head fitted with a close-up attachment, and then digitized using the Polytec Scanning Vibrometer software (version 7.4; Polytec Gmbh) through a data acquisition board (National Instruments, PCI-4451). The experiments were carried out at three ambient temperatures (i.e., 18, 22, and 27 °C), and the experimental chamber was maintained at the desired temperature using a wall mounted air conditioner and room heater. The temperature was monitored using a Testo 110 precision thermometer (Testo Ltd.) at the beginning and end of the measurement, and the measurement was deemed acceptable only if the temperature remained with ±2°C of the desired temperature. Measurements were made across both raised tegmina in a single scan.

Acoustic stimuli. The tegmina of the tree cricket were acoustically stimulated using a loudspeaker positioned exactly below the mounted animal at a distance of approximately 13 cm in all of the experiments. Acoustic stimuli were produced using the Polytec scanning vibrometer software (version 7.4; Polytec Gmbh), amplified (Sony amplifier model TA- E570), and passed to a loudspeaker (Maplin L65AW; Maplin Electronics). Sounds were constantly and simultaneously measured and recorded during the experiment using a calibrated 1/8-inch (3.2 mm) precision pressure microphone (Brüel and Kjær, 4138) and preamplifier (Brüel and Kjær, 2633). The microphone has a flat response in the measured frequency range, and it was positioned approximately 2 mm directly above the tegmina of the animal. Periodic chirps were presented with a bandwidth from 0.5 to 10 kHz (λ: 68.6 to 3.43 cm) at 11 mPa (55 dB re 2×10^{-5} N/m^2). The sound pressure level of the signals was kept constant (±3 dB) over the entire frequency range. Because the loudspeaker was placed exactly below the mounted animal such that the

direction of propagation of the sound was parallel to the faces of the wings, any effect of sound reflected or radiated by the wings was minimized. In addition, the wavelengths of the sounds used were significantly larger than the wing size effectively rendering the incident acoustic field spatially diffuse.

Vibrometric measurements. Analyses of tegminal vibrational velocity and sound pressure level were carried out using the laser control software (Polytec scanning vibrometer, version 7.4 and version 8.5, Polytec GmbH). The velocity of vibration of the wing was sampled simultaneously with the acoustic signal. Averages of 10 responses were made at each point in the scanning lattice, which was placed over the entire tegmina. Using a Fast Fourier transform with a rectangular window, a frequency spectrum was calculated with a resolution of 12.5 Hz. The data were smoothed using a moving average window of 20 points (equivalent to 250 Hz). The laser and microphone signals were then used to calculate the coherence, gain and phase of the responses. The transfer function of the wing displacement with respect to the reference sound level of the acoustic stimulus and the coherence between the vibrometer and the microphone signals were calculated as in Windmill, et al. (49). Data were considered reliable only when the coherence of the transfer function was above 0.8 and was above this value over most of the tegmina. Data were collected from eight individuals.

Finite element analysis of sound radiating wing structures. The resonant behavior of a stiff plate such as the wing can be modeled using an finite element modeling approach. The information required to develop such a model are the geometry and boundary conditions of the plate and the properties of its material. Material properties determine the speed and wavelength of flexural waves produced by a harmonic force driving the material. The geometry and boundary conditions of the plate then determine where these waves reflect, dissipate, and interact. Together these parameters determine the shapes of the resonant modes and the frequencies at which they occur. Damping parameters can also be added to the model in order to produce a more complete picture of the frequency response of the plate that includes the width of the frequency response around each eigenfrequency.

We investigated the contribution of the aspect ratio of the wing to its frequency response. Finite element models were constructed using the software COMSOL Multiphysics (v 4.2, COMSOL AB). The wing was modeled as an isotropic stiff plate, and its modal shapes and FRF in response to sound pressure (at 11 mPa) were investigated. The geometry of the face of the plate was based on measurements made from images of *O. henryi* wings held in the singing position scaled against available data (22). The two plates were then placed at an angle of 5° with respect to each other such that they made contact near the stridulatory apparatus as they would be held during singing (see Fig. S4). The wings were defined as contact pairs which prevented them from interpenetrating during model solving.

The boundary conditions for the plate were estimated as being clamped on all edges based on the modal shapes produced by the real wings. The first mode produced by the wing indicates that the wing edges were immobile; thus, they could be approximated as being clamped. The wing hinge is held rigid during singing; therefore, we concluded that the boundary of the resonator associated with this hinge could be considered clamped. In addition, deflection shape data show that the framework of venation of the wing edges and the subcostal area together keep the edges of the main resonant plate clamped.

The mechanical properties of the wing material are unknown for *O. henryi*. For a stiff plate model, in addition to its geometry, the Young's modulus (E), Poisson's ratio (υ), and density (ρ) of the material were required. Because these properties have not yet been measured, we treated the model as being parametric and reported the ratios of the frequencies of the first two modes rather than absolute frequency. While the mechanical parameters influenced the precise eigenfrequencies of a plate, they did not change their ratio (34). We investigated this relationship over two orders of magnitude of the E, υ, and ρ starting with previously measured values of these for other insect wings ($E = 3.5$ GPa, $\upsilon = 0.3$, $\rho = 1,200$ kg/m^3) (50, 51) (see Fig. S6). We found that the ratio did not change over this range; thus, it is possible to consider that any combination of material parameters used to achieve mode (1,1) at a particular $f(1, 1)$ will also give rise to mode (1,2) at $1.25^{*}f(1, 1)$. In addition, the reliability of the model was established by a study of mesh element number (see Fig. S5) which showed that the model was extremely robust.

We modeled damping using Rayleigh damping parameters which were estimated based on the damping ratio of two modes. A simple harmonic oscillator model was fitted to each of the two modes of the vibrometric frequency responses of the real wing harps. The damping ratio was estimated from the fit. The mass associated (α_{DM}) and stiffness associated damping (β_{DS}) were then estimated by solving the following equation as simultaneous equations for the two wing modes:

$$\zeta_n = \frac{1}{2\omega_n}\alpha_{\mathrm{DM}} + \frac{\omega_n}{2}\beta_{\mathrm{DS}}. \qquad [5]$$

Where, ζ_n is the damping ratio for mode n, ω_n is the angular frequency associated with mode n.

Calculating radiated sound power. We simplified the problem of estimating the sound power radiated by *O. henryi* wings or harps by considering the acoustic power produced by only the first mode of vibration. The first mode in both situations could be readily approximated as a piston vibrating within an infinite baffle. While the standing wave produced in the wings does not produce equal movement across the wing surface like a piston, it did move in phase; consequently, we could use the average motion as an approximation (3, 52). The acoustic power (P_r) radiated by the entire wing or the harp can then be approximated by (39):

$$P_r = R_0\langle|v|^2\rangle. \qquad [6]$$

Where R_o is the structure's radiation resistance in air and v is the time averaged and space averaged normal velocity of the wing. The radiation resistance (R_o) of the two structures is dependent on the match or lack thereof between the wavelength of the radiated frequency in air and the size of the radiating body. R_o is described by the following approximation when $(2k_oa)^2 \ll 1$ (39) as is the case here and with most insects:

$$R_0 = \frac{\rho_0 c_0 S(2k_0 a)^2}{8}. \qquad [7]$$

Where ρo, and c_o are the density of air and speed of sound in air, S is the area of the radiating piston, k_0 is the wave number ($k_0 = \omega/c_o$), and a is the smallest transverse dimension of the radiating piston. Using the density of air and speed of sound at 20 °C (1.2 kg/m^2 and 343.2 m/s, respectively), the area of two wings or two harps combined ($34.2^{*}10^{-6}$ m^2 and $5.2^{*}10^{-6}$ m^2, respectively), and the same a ($4.6^{*}10^{-3}$ m) equivalent to twice the width of the harp for both systems, we calculated the radiation resistance. To estimate k for the two situations, we parameterized our model using realistic values (50, 51) to produce mode 1 at 3 kHz, as in the real wings (see Figs. S5 and S6), and then used the same parameter set to find the first mode of the harps. The harps produce mode 1 at a frequency 3.67 times higher; i.e., 11 kHz. The resulting radiation resistance experienced by the two wings is lower ($4.49^{*}10^{-4}$ N/(m/s)) than that of the harps ($9.189^{*}10^{-4}$ N/(m/s)). This difference in radiation resistance implies that any increase in radiated power produced by the full wings rather than the harps would have to be achieved by increasing the average surface velocity.

We used the same models to estimate the average surface velocity. We increased the pressure applied to the harps by 6.57 times to correct for the difference in area between the full wings and the harps alone thereby effectively applying the same amount of force to the system. The resulting average surface velocity of the full wings is higher at $19^{*}10^{-5}$ m/s than the harps at $8.44^{*}10^{-5}$ m/s. The power radiated by the wings under these conditions is estimated to be greater than that radiated by the harps alone by a factor of 2.5.

ACKNOWLEDGMENTS. N.M. is supported by a Marie Curie fellowship; F.M.-Z. is supported by a Human Frontier Science Program fellowship; and D.R. by a Royal Society Wolfson fellowship. The project was funded by the UK-India Education and Research Initiative and a grant from the Biotechnology and Biological Sciences Research Council.

1. Alexander RD (1967) Acoustical communication in arthropods. *Annu Rev Entomol* 12:495–526.
2. Bennet-Clark HC (1999) Resonators in insect sound production: how insects produce loud pure-tone songs. *J Exp Biol* 202:3347–3357.
3. Bennet-Clark HC (1989) Songs and the physics of sound production. *Cricket Behavior and Neurobiology*, eds F Huber, TE Moore, and W Loher (Cornell University Press, Ithaca), pp 227–261.
4. Bennet-Clark HC (1998) Size and scale effects as constraints in insect sound communication. *Philos T Roy Soc B* 353:407–419.
5. Elliott CJH, Koch UT (1985) The clockwork cricket. *Naturwissenschaften* 72:150–153.
6. Koch UT, Elliott CJH, Schäffner KH, Kleindienst HU (1988) The mechanics of stridulation of the cricket: *Gryllus campestris*. *J Comp Physiol A* 162:213–223.
7. Bennet-Clark HC, Bailey WJ (2002) Ticking of the clockwork cricket: the role of the escapement mechanism. *J Exp Biol* 205:613–625.
8. Bishop JFW (1955) The physics of clocks and watches. *J Sci Instrum* 32:289–293.

9. Jonathan B (1993) John Harrison: inventor of the precision timekeeper. *Endeavour* 17:160–167.
10. Walker TJ (1962) Factors responsible for intraspecific variation in the calling songs of crickets. *Evolution* 14:407–428.
11. Martin SD, Gray DA, Cade WH (2000) Fine-scale temperature effects on cricket calling song. *Can J Zool* 78:706–712.
12. Pires A, Hoy R (1992) Temperature coupling in cricket acoustic communication I. Field and laboratory studies of temperature effects on calling song production and recognition in *Gryllus firmus*. *J Comp Physiol A* 171:69–78.
13. Walker TJ (1962) The taxonomy and calling songs of United States tree crickets (Orthoptera: Gryllidae: Oecanthinae) I. The genus *Neoxabea* and the *niveus* and *varicornis* groups of the genus *Oecanthus*. *Ann Entomol Soc Am* 55:303–322.
14. Simmons LW (1995) Correlates of male quality in the field cricket, *Gryllus campestris* L.: age, size and symmetry determine pairing success in field populations. *Behav Ecol* 6:376–381.
15. Simmons LW, Zuk M (1992) Variability in call structure and pairing success of male field crickets, *Gryllus bimaculatus*: the effects of age, size and parasite load. *Anim Behav* 44:1145–1152.
16. Simmons LW, Ritchie MG (1996) Symmetry in the songs of crickets. *P Roy Soc Lon B* 263:1305–1311.
17. Brown WD, Wideman J, Andrade MCB, Mason AC, Gwynne DT (1996) Female choice for an indicator of male size in the song of the black-horned tree cricket, *Oecanthus nigricornis* (Orthoptera: Gryllidae: Oecanthinae). *Evolution* 50:2400–2411.
18. Brown WD (2008) Size-biased mating in both sexes of the black-horned tree cricket, *Oecanthus nigricornis*; Walker (Orthoptera: Gryllidae: Oecanthinae). *J Insect Behav* 21:130–142.
19. Fitch WT (1999) Acoustic exaggeration of size in birds via tracheal elongation: comparative and theoretical *analyses*. *J Zool* 248:31–48.
20. Fitch WT (1997) Vocal tract length and formant frequency dispersion correlate with body size in rhesus macaques. *J Acoust Soc Am* 102:1213–1222.
21. Walker T (1957) Specificity in the response of female tree crickets (Orthoptera, Gryllidae, Oecanthinae) to calling songs of the males. *Ann Entomol Soc Am* 50:626–636.
22. Metrani S, Balakrishnan R (2005) The utility of song and morphological characters in delineating species boundaries among sympatric tree crickets of the genus *Oecanthus* (Orthoptera: Gryllidae: Oecanthinae): a numerical taxonomic approach. *J Orthop Res* 14:1–16.
23. Sismondo E (1979) Stridulation and tegminal resonance in the tree cricket *Oecanthus nigricornis*; (Orthoptera: Gryllidae: Oecanthinae). *J Comp Physiol A* 129:269–279.
24. Fulton B (1915) The tree crickets of New York: life history and bionomics. *New York Agricultural Experiment Station Technical Bulletin* 42:1–47.
25. Fulton B (1926) The tree crickets of Oregon. *Oregon Agricultural College Experimental Station Bulletin* 223:1–20.
26. Sismondo E (1993) Ultrasubharmonic resonance and nonlinear dynamics in the song of *Oecanthus nigricornis* F Walker (Orthoptera: Gryllidae). *Int J Insect Morphol* 22:217–231.
27. Montealegre-Z F, Jonsson T, Robert D (2011) Sound radiation and wing mechanics in stridulating field crickets (Orthoptera: Gryllidae). *J Exp Biol* 214:2105–2117.
28. Bennet-Clark HC (2003) Wing resonances in the Australian field cricket *Teleogryllus oceanicus*. *J Exp Biol* 206:1479–1496.
29. Montealegre-Z F, Morris GK, Mason AC (2006) Generation of extreme ultrasonics in rainforest katydids. *J Exp Biol* 209:4923–4937.
30. Montealegre-Z F, Mason AC (2005) The mechanics of sound production in *Panacanthus pallicornis* (Orthoptera: Tettigoniidae: Conocephalinae): the stridulatory motor patterns. *J Exp Biol* 208:1219–1237.
31. Prestwich KN, O'Sullivan K (2005) Simultaneous measurement of metabolic and acoustic power and the efficiency of sound production in two mole cricket species (Orthoptera: Gryllotalpidae). *J Exp Biol* 208:1495–1512.
32. Montealegre-Z F, Windmill JFC, Morris GK, Robert D (2009) Mechanical phase shifters for coherent acoustic radiation in the stridulating wings of crickets: the plectrum mechanism. *J Exp Biol* 212:257–269.
33. Fahy F, Gardonio P (2007) *Sound and Structural Vibration: Radiation, Transmission and Response* (Academic Press, Elsevier, Oxford, United Kingdom), 2nd Ed.
34. Rossing TD, Fletcher NH (1994) *Principles of vibration and sound* (Springer-Verlag Inc., New York).
35. Foster JA, Robertson RM (1992) Temperature dependency of wing-beat frequency in intact and deafferented locusts. *J Exp Biol* 162:295–312.
36. Xu H, Robertson RM (1994) Effects of temperature on properties of flight neurons in the locust. *J Comp Physiol A* 175:193–202.
37. Souroukis K, Cade WH, Rowell G (1992) Factors that possibly influence variation in the calling song of field crickets: temperature, time, and male size, age, and wing morphology. *Can J Zool* 70:950–955.
38. Bennett AF (1984) Thermal dependence of muscle function. *Am J Physiology—Reg I* 247:R217–R229.
39. Hambric SA, Fahnline JB (2007) Structural acoustics tutorial-part II: Sound-structure interaction. *Acoustics today* 3:9–26.
40. Farris HE, Forrest TG, Hoy RR (1997) The effects of calling song spacing and intensity on the attraction of flying crickets (Orthoptera: Goryllidae: Nemobiinae). *J Insect Behav* 10:639–653.
41. Forrest TG, Raspet R (1994) Models of female choice in acoustic communication. *Behav Ecol* 5:293–303.
42. Forrest TG (1994) From sender to receiver: propagation and environmental effects on acoustic signals. *Integr Comp Biol* 34:644–654.
43. Bussière LF, Clark AP, Gwynne DT (2005) Precopulatory choice for cues of material benefits in tree crickets. *Behav Ecol* 16:255–259.
44. Brown W (2011) Allocation of nuptial gifts in tree crickets changes with both male and female diet. *Behav Ecol Sociobiol* 65:1007–1014.
45. Hedrick A (2005) Environmental condition-dependent effects on a heritable, preferred male trait. *Anim Behav* 70:1121–1124.
46. Magnuson JJ, Crowder LB, Medvick PA (1979) Temperature as an ecological resource. *Am Zool* 19:331–343.
47. Hartmann WH (1998) *Signals, Sound and Sensation* (Springer Verlag, New York).
48. Prestwich KN, Lenihan KM, Martin DM (2000) The control of carrier frequency in cricket calls: a refutation of the subalar-tegminal resonance/auditory feedback model. *J Exp Biol* 203:585–596.
49. Windmill JFC, Gopfert MC, Robert D (2005) Tympanal travelling waves in migratory locusts. *J Exp Biol* 208(1):157–168.
50. Song F, Lee KL, Soh AK, Zhu F, Bai YL (2004) Experimental studies of the material properties of the forewing of cicada (Homoptera, Cicadidae). *J Exp Biol* 207:3035–3042.
51. Smith CW, Herbert R, Wootton RJ, Evans KE (2000) The hind wing of the desert locust (*Schistocerca gregaria* Forskal). II. Mechanical properties and functioning of the membrane. *J Exp Biol* 203:2933–2943.
52. Fletcher NH (1992) *Acoustic systems in biology* (Oxford University Press, New York).

Supporting Information

Mhatre et al. 10.1073/pnas.1200192109

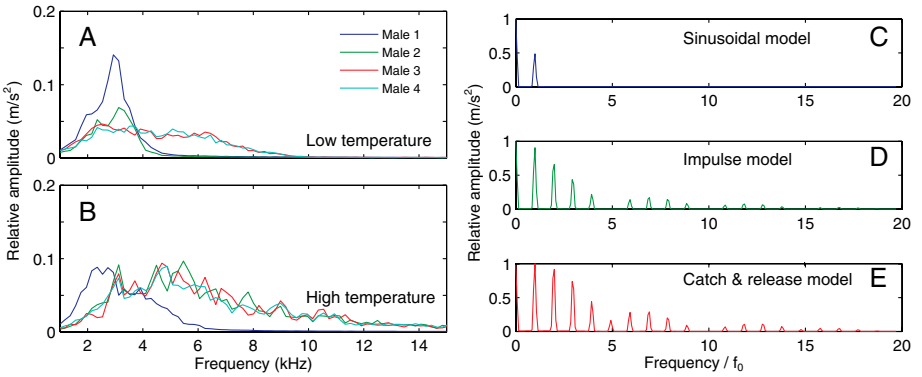

Fig. S1. Frequency spectra of the acceleration observed in five closing wing strokes at (*A*) low, (*B*) high temperatures and of the expected behavior from three different escapement models, (*C*) the sinusoidal model, (*D*) the impulsive force model, and (*E*) the catch and release model. (*A*) At low temperatures, two of the males have nearly tonal force spectra, which are similar to the (*C*) sinusoidal model; however, two males already show the presence of harmonics as expected from the other two models. (*B*) At higher temperatures, three males show clear evidence of higher harmonics, whereas the harmonics are suppressed in one male. In the real data, the relative amplitude of the harmonics is smeared more than it is in the model data. The broadening of the harmonics is probably caused by imperfect periodicity in the peg strikes. Additional smearing is caused by deviations in the waveform from the expected pulse-like behavior (plotted in Fig. 3*A*). Thus, the frequency data supports the time domain data suggesting a flexible drive system that varies between a pure sinusoidal drive and an imperfect escapement drive.

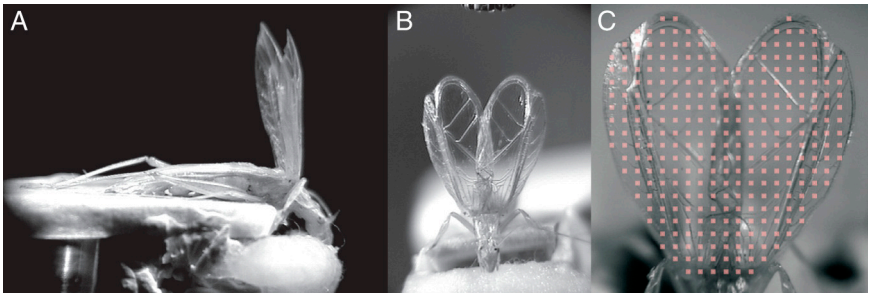

Fig. S2. Images of the mounted animal (*A*) side and (*B*) front view, and (*C*) scan points on the wings in a singing position.

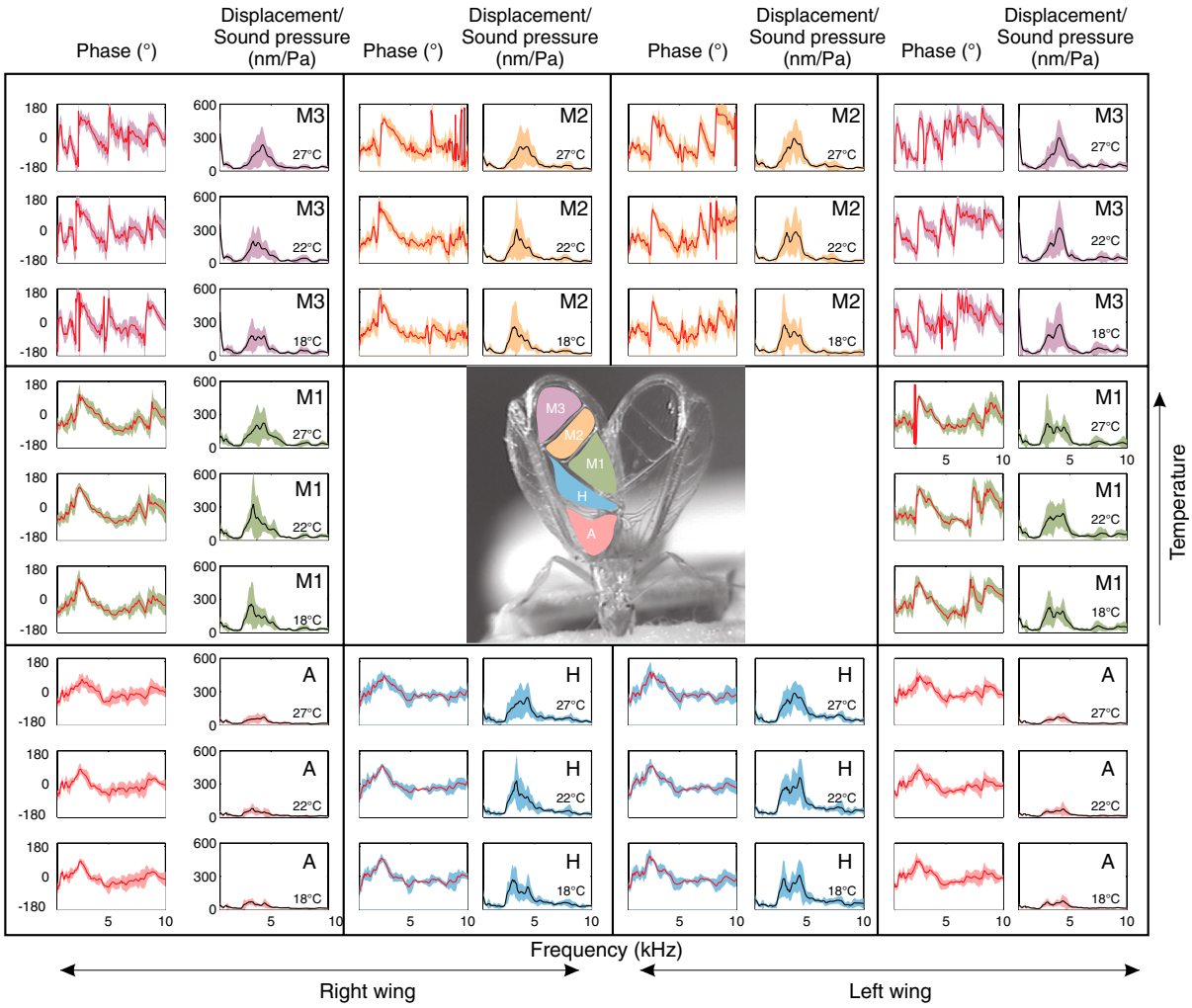

Fig. S3. The amplitude and phase of the displacement transfer function measured at different wing areas at three different temperatures. The amplitude response in the anal field (*A*) is the lowest, and all other areas the harp (*H*) and mirror 1, 2, and 3 (*M1*, *M2*, *M3*) vibrate at higher amplitudes in response to sound. The amplitude and phase responses of all wing areas show signs of the two observed modes. In the amplitude response, it is indicated by two closely placed peaks. In the phase response, it is indicated by the step-like shape observed in the phase transition from +90° to −90°.

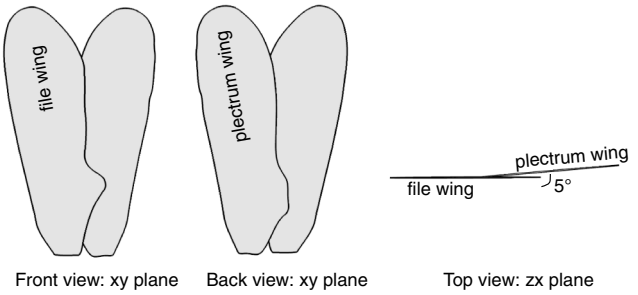

Fig. S4. The 3D geometry used to model the wings.

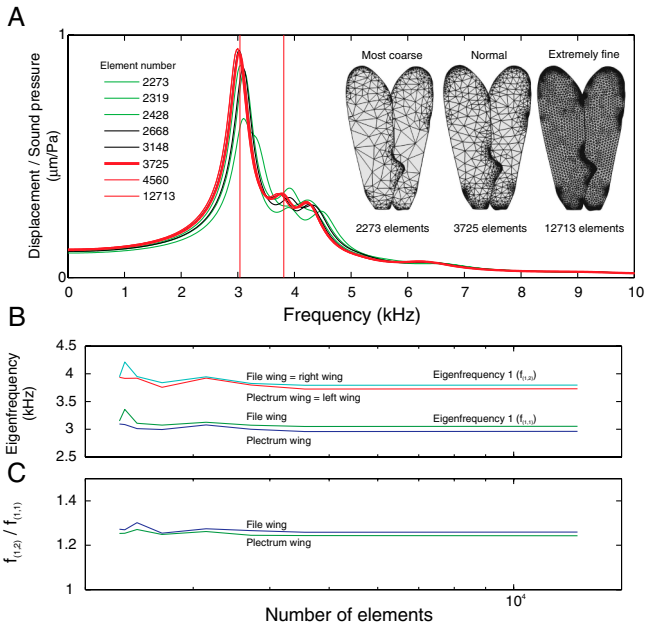

Fig. S5. A study on the effect of mesh element number on frequency response and eigenfrequency. (*A*) The average frequency response of the modeled wings solved at different element numbers do not vary greatly with the number of elements used in the finite element (FE) model except at the lowest element number. Similarly, (*B*) the eigenfrequencies and (*C*) their ratios are not greatly affected by the element number except at the lowest element numbers. The greatest difference is seen in the least element number model where the relative displacement amplitudes of the two modes are misrepresented. This difference reflects the mismatch seen between the model average frequency response, where many elements were effectively measured from, and that seen from the measurements where far fewer scan points were measured from. The number of elements correspond to COMSOL physics controlled mesh categories with the highest being extremely fine then, in descending order, finer, normal, coarse, coarser, extra coarse, and extremely coarse. The lowest was made by further reducing the mesh element number by manipulating the mesh characters manually because COMSOL did not have a lower mesh size category. The mesh size normal is used for all other FE models in this manuscript. (*A*) Also plotted is the average of the first two eigenfrequencies of the two wings as solved for the normal mesh size, which indicates the location of the first modes in the frequency response. Studies of other parameters used in the FE model, such Young's modulus and Poisson's ratio, use the normal mesh size and report only the average of the first two eigenfrequencies of the two wings, the frequencies of the $f(1, 1)$ and $f(1, 2)$ modes (*A*) rather than the entire frequency response.

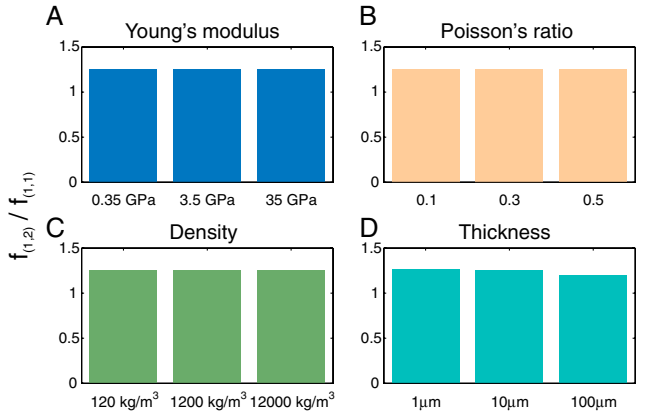

Fig. S6. The effect of FE model parameters on the ratio of the first two eigenfrequencies. The first eigenfrequency for each wing was calculated and the average taken across the two wings. A similar procedure was followed for the second eigenfrequency. The first two eigenfrequencies corresponded to the $f(1, 1)$ and $f(1, 2)$ mode in all models. Each parameter under investigation varied (*A*) the Young's modulus, (*C*) the density, and (*D*) the thickness of the modeled wings varied over three orders of magnitude. The Poisson's ratio for most materials lies between 0.2–0.3 within the elastic region. In some soft biological materials, this ratio may increase up to 0.5. (*B*) Hence, the Poisson's ratio was varied within this limit from 0.1–0.5. As expected, we found that changing the Young's modulus, Poisson's ratio, and density does not change the ratio of the first two eigenfrequencies. The effective stiffness of a plate changes faster than the effective mass as its thickness increases; hence, it is an important parameter to investigate. We found that changing the thickness of the thin plate over two orders of magnitude has a small, though not significant effect on the ratio of the two eigenfrequencies. Thus, we showed that the geometry of wing and its aspect ratio is the character that is significant to the merging of the first two resonant modes in the frequency domain. The central parameters in all cases produce a model that matches the eigenfrequencies of the real wings, and they are reasonable based on previous measurements from the wings of other insects (1–3). The central parameter values are used in the element number study and for each parameter study except for the varied parameter.

1 Song F, et al. (2004) Experimental studies of the material properties of the forewing of cicada (Homoptera, Cicadidae). *J Exp Biol* 207:3035–3042.
2 Smith CW, et al. (2000) The hind wing of the desert locust (*Schistocerca gregaria Forskal*). II. Mechanical properties and functioning of the membrane. *J Exp Biol* 203:2933–2943.
3 Vincent JFV, Wegst UGK (2004) Design and mechanical properties of insect cuticle. *Arthropod Structure & Development* 33:187–199.

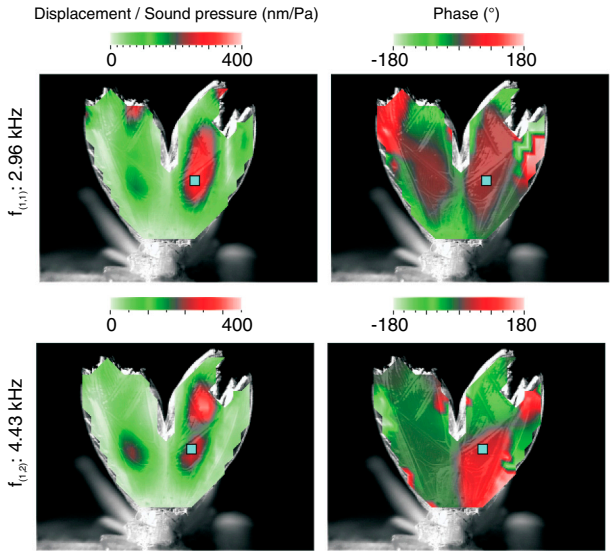

Fig. S7. The damaged wings of an *O. henryi* male show resonant modes similar to those seen in undamaged wings.